Diffusive methane burst during a blue tide, wind-driven event in a meromictic lake

Masafumi Sasaki [a], Keisuke Nakayama [b*], Yasuyuki Maruya [c]

[a] Department of Mechanical Engineering, Kitami Institute of Technology, Koencho-165, Kitami, 090-8507, Japan

[b] Graduate School of Engineering, Kobe University, 1-1 Rokkodai-Cho Nada-Ku, Kobe 658-8501, Japan

[c] Graduate School of Engineering, Kyushu University, 744 Motooka, Nishi-Ku, Fukuoka 819-0395, Japan

*Corresponding author: Keisuke Nakayama, Tel.: +81-78-803-6056
Email: nakayama@phoenix.kobe-u.ac.jp

Abstract: Strong stratification has formed in Lake Abashiri, a typical meromictic lake in Hokkaido, in the subarctic zone in Japan. When the anoxic water of the lower layer is upwelled to the surface by a strong wind, fish and corbicula clams die due to a lack of dissolved oxygen. This event is called as blue tide. It was observed that the dissolved methane in the lake decreased more than 100 t after the blue tide which occurred in 2008. This is the discovery of the phenomenon that a large quantity of methane diffuses to the atmosphere caused by upwelling of anoxic water which contains dissolved methane. We named the event as "methane burst". It is also the first report that the wind-driven upwelling is reproduced using a numerical analysis code and the methane burst is analyzed. During this blue tide, the methane flux was approximately 170 times greater than usual.

----

* Corresponding author. E-mail: nakayama@phoenix.kobe-u.ac.jp (Keisuke Nakayama)

1 Introduction

Maritime lakes (lagoons) are often stratified by seawater and fresh water flowing into them. When the residence time of the seawater in a maritime lake is sufficiently long, an anoxic (low dissolved oxygen concentration) saline layer forms below the upper freshwater layer as the accumulated organic matter over the bottom sediment consumes oxygen in the lower layer. The stratification prevents oxygen replenishment and results in permanently anoxic lower saline layer waters, but strong winds sometimes cause the upwelling of anoxic saline water to the surface. The wind-driven upwelling of anoxic waters, including sulfides, causes noxious odors and damages fisheries by killing fish and corbicula clams. This event is called as blue tide. Blue tide events are observed in not only such meromictic lakes but also lagoons filled with seawater (e.g., Lake Notoro; Yamamoto et al., 2009), semi-enclosed bays (e.g., Tokyo Bay; Sasaki et al., 2009), brackish water near the mouths of rivers (e.g., Megro River; Miura et al., 2009), and freshwater lakes (e.g., Bacaniov et al., 2014; Finlay et al., 2001; Macintyre et al., 1999; Reynolds, 2006; Spigel and Imberger, 1980).

Lake Abashiri, located in Hokkaido, Japan's northernmost and subarctic island, is a typical meromictic (brackish) lake that is also known to be highly eutrophic. The water column (with a maximum depth of 16.8 m) became permanently stratified with an upper freshwater layer and a lower saline layer in the 1920s. The boundary between the freshwater and saline layers became rapidly more shallow (approximately 6 m), especially in the 1980s as a large quantity of seawater flowed into the lake because of the stream bed digging at the mouth of the outflow river. A blue tide was first observed at Lake Abashiri in 1987 and has recurred most years since then (Ministry of Land, Infrastructure, Transport, and Tourism, 2007). However, the frequency of blue tides in Lake Abashiri has recently decreased due to successful efforts to deepen the saline boundary by the office of Development and Construction Department of Abashiri, MLIT (Ministry of Land, Infrastructure, Transport, and Tourism). However, blue tides have happened a few times since 2019, as strong winds frequently occur due to climate change (Nakayama et al., 2010).

Three mechanism that methane is released from the surface of a stratified lake to the atmosphere is diffusion, ebullition and plant mediated emission (Bastviken, et al, 2004). Of these, we intend only for diffusion in this article. A simple model of air-sea diffusion (gas exchange) mechanism was proposed as two-film model by Liss and Slater (1974). Enormous studies on the transfer coefficient have been carried out afterwards. Ebullition is a phenomenon that bubbles containing methane are released directly from the bottom of a lake to the atmosphere. It is thought that there happens ebullition in Lake Abashiri also. However, ebullition could not be observed by the method in the present study.

Sasaki and Endoh (2014) reported an inverse relationship between dissolved methane concentration (DM) and lake area (A) for 12 major lakes in Hokkaido. The average DM in Lake Abashiri showed a remarkable divergence from the average DM vs. A trend in Hokkaido and European boreal lakes (Bastviken et al., 2004; Juutinen et al., 2009). Therefore, we carried out field observations of DM in Lake Abashiri from 2005 to 2013. Field observations by Maruya et al. (2013) showed that the anomaly of DM on the surface of Lake Abashiri might be caused by diffusion from very high DM in the saline layer. Moreover, Maruya et al. (2022) inicated that methane production from bottom sediment could be estimated by a logistic function model with DO concentrations in water overlying the bottom. Dissolved methane at the saline layer is transported to the upper layer with a saline water by the wind driven convection and turbulence diffusion. Therefore, methane accumulated in the saline layer of Lake Abashiri is transported to the upper freshwater layer, and it is expected that a large amount of methane will diffuse to the atmosphere during a blue tide. We call the phenomenon as (diffusive) "methane burst". In the present study, we estimated the quantity of methane transported by wind-driven convection and turbulence from the saline layer to the

freshwater layer using the Fantom environmental fluid dynamics model (Nakayama et al., 2012; Nakayama et al., 2014; Nakayama et al., 2020a). The magnitude of the diffusive methane burst was estimated, and the results were verified by field observations when a blue tide occurred on November 8, 2008.

2 Materials and methods
2.1 Site description and characteristics of Lake Abashiri
Hokkaido, the northernmost island of Japan, is located in the subarctic region, and most of the lakes in Hokkaido are covered with ice in the winter. Lake Abashiri, shown in **Fig. 1**, has a surface area of 32.3 km^2 and a maximum depth of 16.8 m. Lake Abashiri is highly eutrophic due to the anthropogenic influence of livestock and agriculture in its basin. The main inflow river is the Abashiri, which accounts for 97% of the inflow, and the outflow runs to the Okhotsk Sea through a river length of 7.2 km. Therefore, oceanic water flows into the lower layer of the lake depending on the tide (Nakayama et al., 2016), resulting in strong stratification.

2.2 Procedures for water sampling and DM analysis
The locations of observation stations are shown in **Fig. 1**. The stations include seven offshore stations (circles), seven onshore stations (triangles), and two other stations (squares) along the Abashiri River near the inlet to Lake Abashiri. The northernmost station at the outlet mouth of the Abashiri River (outflow) is represented by Station (St.) LA3. Surface water samples were obtained at the offshore stations using a stainless-steel pail from the observation boat 'Aosagi' of MLIT. At St. 5 (maximum depth), water samples were obtained from nine different depths by using a Van Dorn water sampler (2 L) to determine the vertical *DM* distribution throughout the water column. Data for the vertical profile of salinity (*S*) and of the dissolved oxygen concentration (*DO*) at St. 5 were obtained from the office of the Development and Construction Department of Abashiri, MLIT.

Salinities were measured by an electric conductivity method using a conductivity and temperature depth sensor (CTD). Each water sample was sealed in a 500 mL glass bottle. A part of the water sample from each bottle in three small vials (27 mL each) was replaced by nitrogen, leaving 10 mL of sample in each vial. After each vial sample had been heated and kept at 60°C for more than 20 minutes, 1.625 mL of headspace gas was injected into a gas chromatography system (Shimadzu GC-14B) equipped with a flame ionization detector. The sampling and *DM* analysis procedures were described in detail by Sasaki et al. (2010). Since all samples in this study were analyzed within 12 hours of collection, no preservative was added to the water samples. The average *DM* at the lake surface was obtained as an area-weighted mean. The lake surface was divided into several sections, where each station was located near the center of a section. When the flux of diffusive methane was calculated from the measured *DM* data, the on-shore area and the off-shore area were divided into 6 and 3 sections, respectively. As the mean freshwater layer depth was usually about 6 m, the on-shore area was defined as the area shallower than 6 m (the nominal depth of the freshwater layer).

2.3 Cultivation tests of water samples in an incubator
A part of methane in oxic water is likely oxidized by methane-oxidizing bacteria (Bastviken et al., 2002). Cultivation tests of freshwater samples (at the surface of station LA8 on June 28, 2010) and saline water samples (at a depth of 10 m at St. 5 on November 26, 2012) in an incubator were carried out to determine the time-series changes in *DM* caused by oxidation or biochemical decomposition and methanogenesis. Thirteen 500 mL glass bottles were used for freshwater sampling, and thirteen 125 mL glass vials were used for saline water sampling.

DM was measured every week for approximately 1 month under cold (5°C) and warm (30°C) conditions with and without light. The intensity of light radiation was controlled by lamps set to be the same as the average daily global radiation in Abashiri for the past decade, i.e., 150 W m^{-2}.

2.4 Numerical fluid analysis for the transportation of DM

Fantom, an environmental fluid dynamics model developed by one of the authors (Nakayama et al., 2012), was used to analyze the characteristics of stratified flows, such as the upwelling of the lower layer to the water surface (Shintani et al., 2010) and the breaking of internal waves over a uniform slope (Nakayama and Imberger, 2010). Fantom is an object-oriented hydrodynamic model (written in C^{++}) intended to simulate transport phenomena under a stratified condition (Maruya et al., 2010). The computational scheme is similar to the predictor-corrector method shown in Nakayama (2006), which analyzed stratification effects on flows. A three-dimensional Boussinesq-type equation and mass conservation were applied. This study used a generic length-scale turbulent closure model, k-e (Umlauf and Burchard, 2003), with a CA filter (Warner et al., 2005). The advection scheme for momentum and scalar was ULTIMATE QUICKEST (Leonard, 1991), while a first-order upwind scheme was used for subgrid-scale turbulent kinetic energy to achieve numerical stability by including numerical diffusion. Fantom was able to satisfactorily reproduce the observed time-series vertical distributions of salinity at three stations for 30 days in Lake Abashiri (Maruya et al., 2010). Residual currents due to the breaking of internal waves in a two-layer field in laboratory experiments were also reproduced using Fantom (Nakayama et al., 2019 and Nakayama et al., 2020b). Since these results successfully reproduced the observed results, Fantom was also applied in this study to the blue tide that occurred in Lake Abashiri in 2008. The mesh size in the vertical direction (z-axis) was 0.15 m, and there were 151 meshes in total (including atmospheric elements beyond the water's surface). The mesh size in the horizontal direction was 200 m, and there were $i = 1\sim27$ and $j = 1\sim55$ meshes in the x and y directions, respectively. The total number of elements was 224,235. The time step was 40 s. The lake volume was divided into four subdomains, and parallel processing was executed with a four-core personal computer.

The freshwater and saline water boundary depth d_B was 4.6 m based on salinity observations in 2008. Since a blue tide in Lake Abashiri was observed on November 8, 2008, the analysis period was set to 20 days from November 5. The initial distributions of salinity S, *DM* (bottom-shape-traced distribution), *DO*, and water temperatures were obtained from observations on September 29. The vertical dissolve methane concenttration (*DM*) profile at the lake's center did not vary from June 30 to September 29 (as shown in Section 3.1). Therefore, September 29 is considered the representative and typical methane condition in Lake Abashiri.

Fantom requires data for wind speed (m s^{-1}), wind direction (degrees), air temperature (°C), relative humidity (%), short wave emission (W m^{-2}), atmospheric pressure (Pa), the flow rate of the river (m^3 s^{-1}), and rainfall (mm hr^{-1}). Data for hourly wind speed (U_2 at a height of 2 m from the water surface) and wind direction obtained by an automatic observatory buoy in the center of the lake (St. 5: point of maximum depth) were corrected to U_{10} (10 m in height) by using a power law, Eq. (1) (Touma, 1977). In the equation, $1/a$ expresses roughness on the ground. It was assumed that $a = 7$ because there were no obstacles such as large trees or buildings.

$$U_{10} = U_2(10/2)^{1/a} = 1.26U_2 \tag{1}$$

Most of the correct values of U_{10} at the center of the lake were higher than those at the AMeDAS (Automated Meteorological Data Acquisition System) station in Abashiri (http://www.jma-net.go.jp/abashiri/index.html) during the blue tide in 2008.

The transfer coefficient k_{600} expressed by an empirical equation, Eq. (2), depending on the wind speed proposed by Cole and Caraco (1998) for CO_2 diffusion from lakes, was applied to estimate methane diffusion during the blue tide event. The diffusive methane flux was calculated simultaneously with flow fields and the other mass transport computations. The transfer coefficient of methane k_{CH4} can be obtained by Eq. (3). The Schmidt number of methane Sc_{CH4} depends strongly on water temperature. The mass flux can be calculated by Eq. (4). For more details on estimating the air-lake exchange of methane, refer to Sasaki et al. (2010).

Cole & Caraco equation:
$$k_{600} = 5.75 \times 10^{-6} + 0.597 \times 10^{-6} U_{10}^{1.7} \tag{2}$$

$$k_{CH4} = k_{600}(Sc_{CH4}/600)^{-n} \tag{3}$$

$$f_{mij} = M_{CH4} k_{CH4} A_{ij}(DM_{ij} - DM_0) \tag{4}$$

Where, f_{mij} is the mass flux of methane per lake (g yr^{-1}) , i and j are the element numbers in the x and y directions, respectively, M_{CH4} is the molecular weight of methane, DM_0 is the atmospheric equilibrium dissolved methane concentration, and $n = 0.5$ for higher wind speed field ($U_{10} \geqq 3.6$ m s^{-1}) (Sasaki et al., 2016). We call the methane flux per unit area (f_{mij} / A_{ij}) as a methane flux density (g yr^{-1} m^{-2}).

3 Results
3.1 Observed characteristics of Lake Abashiri
The vertical distribution of salinity S at St. 5 (the lake's center) in 2008 is shown in **Fig. 2a**. There is a clear halocline at a depth of approximately 4.5 ~ 6.5 m. The saline layer (maximum salinity $S = 20$~22 psu) is permanently anoxic water (dissolved oxygen concentration $DO = 0$), as shown in **Fig. 2a**. The reason why DO at the lake surface on Nov. 25 is higher than usual (in June ~ September) is because water temperature lowered. These DO are equivalent to saturated values at the water temperatures. The temperature data at the surface (0.5 m deep) of the lake is shown on the symbol table in **Fig. 2a**. The vertical distribution of DM at St. 5 is shown in **Fig. 2b**. DM and salinity conspicuously increase with depth in the saline water column, while there is no DO in the saline layer. Similar distributions of DM are sometimes observed in small freshwater lakes during summer stratification (Bastviken et al., 2008). Since the latest DM data before the blue tide were obtained on September 29, the data (including DO and S) on that date were used as the initial values of numerical simulations as mentioned above (Section 2.4). The limnological characteristics at St. 5 on September 29 are shown in **Table 1**. The depth of the halocline was approximately 4.6 m on this day.

The results of the cultivation of the freshwater and saline water samples in an incubator are shown in **Fig. 3**. As shown in **Fig. 3** (dashed line), neither a decrease in dissolved methane concentration (DM μmol L^{-1}) caused by oxidation nor an increase in DM by production under reducing conditions was observed for the saline water samples. Therefore, in the following numerical computations, it was unnecessary to consider production due to the methanogen and oxidation of methane in the saline layer. Since the saline water samples smelled like H_2S, it was thought that methanogenesis was inhibited due to the activity of sulfate-reducing

bacteria (Watson and Nedwell, 1998). Additionally, since the lower layer is entirely anaerobic (Maruya et al., 2010), sulfate-reducing bacteria exist in sediments and reduce sulfate to hydrogen sulfide (Boetius et al., 2000; Postgate, 1979). Capone and Kiene (1988) and Minami et al. (2012) revealed that methane production is dominant in sediments under anaerobic conditions where sulfate-reducing bacteria are less active. Thus, the mass balance of methane can be remarkably simplified.

On the other hand, the dissolved methane concentration (DM nmol L^{-1}) in the freshwater column was drastically reduced by oxidation during the night (without sunlight), as shown in **Fig. 3** (solid lines). According to the results of the cultivation of freshwater, the oxidation rate R_{DM} (1 month^{-1}) depends more firmly on solar radiation than on temperature.

$$\text{With solar radiation:} \quad R_{DMwl} = \exp(-0.0145 \Delta t_{wl}) \tag{5}$$

$$\text{Without solar radiation:} \quad R_{DMwol} = \exp(-0.0923 \Delta t_{wol}) \tag{6}$$

Δt_{wl} and Δt_{wol} in Eqs. (5) and (6) are daylight and nondaylight days during the calculation period, respectively. Anaerobic saline water transported to the upper layer is mixed with freshwater (almost in equilibrium) in DO. Therefore, the oxidation of DM by Eqs. (5) and (6) should be considered in the methane mass balance in the freshwater layer. Using a function in Fantom, methane storage in the saline layer was calculated during the open water period in 2008, estimated from the measured DM vertical distribution in **Fig. 2b**, is shown by solid circles in **Fig. 4**. The maximum methane storage was 312 t on September 29. Since there is neither methanogenesis nor oxidation in the saline water column as described above, an increase in DM can be attributed only to dissolution from the sediment at the bottom. A decrease in DM is caused only by the transportation of dissolved methane from the saline layer to the freshwater layer. During the open water season, methane storage usually does not significantly change by the season, as seen from June to September in **Fig. 4**. However, 117 t (= 312 – 195) of dissolved methane disappeared from the saline layer from September 29 to November 25, as shown in **Fig. 4**. Such a significant loss is thought to have occurred with the blue tide on November 8, 2008.

3.2 Methane transportation from the saline layer to the freshwater layer
The numerical simulation started at 0:00 JST on November 5, when the wind speed was sufficiently low before the event. A cross-sectional view of the calculated DM and velocity distributions at 21:00 on November 8, when the maximum hourly wind speed (NNW 19.7 m s^{-1}) was observed during the blue tide, is shown in **Fig. 5b**. The arrow scale shows flow speed (0.1 m s^{-1}). The figure shows the upwelling of the saline water, decline of the boundary, complex convection, delamination of DM along the pycnocline, and transportation of DM to the water surface. The flow speed of x-y axis of the water is largest in near pycnocline of DM and the direction is reverse to the direction of the wind. In contrast with this, the flow near the bottom of the lake is calm. The plane view of DM distributions on the lake surface simultaneously is shown in **Fig. 5a**. As a result of the upwelling of anoxic saline water to the lake surface near the upwind lakeshore, there was a high-DM (approximately 80 µmol L^{-1}) region on the lake surface. The methane transported from the saline to the freshwater layer can be calculated as the total production of DM and the volume in the freshwater layer. The total methane storage is shown in **Fig. 6**. Approximately 105 t of methane was transported to the freshwater layer during the blue tide event (November 5 ~ 12), and 141 t was transported between November 5 and 25. The result is similar to the observations shown in **Fig. 4** for the 26-day period September 29 to November 25 after a blue tide event in which 117 t of methane

disappeared from the saline layer. **Fig. 7** shows the vertical distribution of *DM* calculated at 17 days after the analysis (corresponding to November 25). Because the calculated *DM* vertical distribution in the saline layer (dashed line) resembled an abnormal profile of the distribution observed on November 25, we can infer that this analysis could accurately describe a blue tide event. The d_B became approximately 8 m at the end of the blue tide event, from the initial 4.6 m. The vertical profiles of *DM* also agree well with the calculated value in **Fig. 7**. Thus, we conjecture that the disappearance of a large quantity of methane was caused by diffusion from the lake surface to the atmosphere.

3.3 Estimation of methane flux to the atmosphere during the blue tide event
The changes in methane flux to the atmosphere from November 5 to 25 are shown in **Fig. 8**. The maximum flux appeared under the condition of maximum wind speed and extended to approximately 3.7 t hr^{-1}. The accumulation of methane diffusion to the atmosphere is found by integrating the methane flux in **Fig. 8**. A cumulative amount of 90 t of methane was diffused to the atmosphere during several days (November 8 ~ 12) and substantial amount for this short period. It corresponds to 86% (90 / 105) of the methane quantity transported from the saline to the fresh water.

As a result of mass diffusion to the atmosphere, *DM* of the freshwater layer decreased significantly, as shown in **Fig. 7**. However, the calculated *DM* value in the freshwater layer (= about 4.5 µmol L^{-1}) was more significant than the observed value (= about 0.22 µmol L^{-1}). In the numerical simulations, there was no process in which *DM* disappears from the lake other than diffusion to the atmosphere. There may be two other mechanisms by which *DM* is exhausted from the freshwater layer other than such diffusion. One mechanism is dilution by the inflow from the Abashiri River. The average inflow from the river in November 2008 was 9 m^3 s^{-1} (Ministry of Land, Infrastructure, and Transport and Tourism / Hydrological & Water Quality Database: http://www1.river.go.jp/contents.html). The total quantity of inflow from November 8 to 25 was about 13×10^6 m^3. Since this is equivalent to less than 10% of the volume of the freshwater layer, the inflow of the river has a minimal effect on *DM* in the freshwater layer.

The other mechanism is the aerobic oxidation of methane within the freshwater layer. Assuming the ratio of night and day was 1:2 during the 17-day period (November 8 to 25) using Eqs. (5) and (6), the decline rate of the aerobic resolution was 0.72. This is equivalent to 1.26 µmol L^{-1} when using 4.5 µmol L^{-1}, which was the calculated value for November 25 as the initial value of *DM* in the freshwater layer. Even if this value considers oxidation, it is still higher than the observed value (0.22 µmol L^{-1}). Further study on the mechanism that *DM* in the fresh water layer is settled down to usual level after the blue tide rapidly is necessary.

3.4 Distributions of DM and DO at the water surface
The distributions of *DM* and *DO* at the water surface are shown in **Fig. 9**. The change in the horizontal distribution of *DM* (stars in **Fig. 8**) is shown in **Figs. 9a-c** at 22:00 on the 7th, 4:00 on the 9th, and 24:00 on 10th of November 2008. A strong upwelling of methane was observed near the upwind lakeshore (near the northwest beach). When the wind slowed, the diffusion calmed rapidly. The change in the horizontal distribution of *DO* is also shown in **Figs. 9d** at 22:00 on the 7th, **9e** at 4:00 on the 9th, and **9f** at 24:00 on the 10th of November 2008. Abnormally low *DO* (approximately 4 mg L^{-1}) appeared on the surface during the maximal wind velocity, the same as the highest *DM*. The upwelling of anoxic waters, including sulfides, sometimes kills fish and corbicula clams.

The reason why *DO* near the lake surface on November 25 in **Fig. 2a** is higher than usual (in June ~ September) is because water temperature lowered as mentioned in Section 3.1. Higher salinity than usual in the upper freshwater layer on November 25 suggests that influence of

the transportation of saline water from the lower layer at the blue tide remains, because salinity does not exchange with the atmosphere.

Discussion
4.1 Methane burst due to blue tide
According to the numerical simulations, the dissolved methane transported to the freshwater layer was approximately 105 t during the blue tide in 2008 (during several days) and was 141 t from November 5 to 25. These results agree with the field observation that more than 117 t (312 – 195) of methane disappeared from the saline layer from September 29 to November 25. The vertical distribution of DM at the lake's center after the blue tide, as simulated by Fantom, agreed with the observed profile at least in deeper layer than the d_B on November 25. These suggested that numerical fluid analysis is helpful for estimating transportation (convection and mixing phenomena) even in a permanently stratified meromictic lake such as Lake Abashiri. A large portion (86%) of the methane transported from the saline layer to the freshwater layer was diffused to the atmosphere from Lake Abashiri during several days of the blue tide in 2008.

It is thought that there happens ebullition in Lake Abashiri also. We have ever seen bubbles in lake ice in winter. Since the initial methane storage was count from only dissolved methane measurement, however, ebullition could not be observed in this method.

4.2 Effects of the depth of the epilimnion and saline layer on blue tide outbreaks
Calculations of the virtual boundary depths, $d_B = 6.6$ m, were carried out to determine how d_B influenced the blue tide outbreak. At the start of the calculation, the maximum DM was the same for $d_B = 4.6$ m. The distributions of DM and DO for $d_B = 6.6$ m at the water surface at 4:00 on November 9 2008 are shown in **Fig. 10**. When the boundary depth d_B increases, the reduction of DO is suppressed under the same wind speed condition. In other words, upwelling motions depend sensitively on d_B. The blue tide did not occur under the same wind conditions as the blue tide in 2008, when d_B became deeper by only 2 m. A blue tide was not observed for 6 years after 2009. This is attributed to the deepening of d_B by a gate installed near the Abashiri River outlet by the Development and Construction Department of Abashiri, MLIT. The gate is closed during high tide to prevent oceanic water from entering the lake, and it is opened during ebb tide to allow outflow from the lake.

An increase in the depth of the freshwater boundary (d_B) after the blue tide was found by both the calculations and observations (**Fig. 7**). This suggested that a blue tide is unlikely to occur just after the previous blue tide. It is also expected that a blue tide might be prevented when the lake's level, $i.e.$, the epilimnion thickness, increases due to heavy rain.

4.3 Impact of blue tides on global warming
Since the Abashiri area is not very windy (with an annual average wind velocity of less than 3 m/s), methane fluxes are not very high in an average year. The mean flux density from lakes in Hokkaido is 0.718 g CH_4 yr^{-1} m^{-2} (equal to the value of lakes in Northern Europe; Bastviken et al., 2004), but methane flux from Lake Abashiri is approximately 2~3-times larger at 2.029 g CH_4 yr^{-1} m^{-2} (Sasaki and Endoh, 2014). In contrast, in the case of the blue tide in 2008, since the methane flux during 3 days was approximately 90 t, the annual average flux density corresponded to 342 g CH_4 yr^{-1} m^{-2}, 170 times greater than average. Thus, this phenomenon is good if we call it "methane burst". As the annual methane flux from Lake Abashiri in an average year is 66 t CH_4 yr^{-1}, the 3-day blue tide in 2008 released significantly more methane into the atmosphere than is released in an entire average year. Therefore, a blue tide driving a methane burst can be described as an extreme event that is attributable to

climate change. In contrast to a stratified meromictic lake, strong stratification also accumulates higher *DM* in the lower layer of a eutrophic freshwater lake, and methane may be released due to the upwelling of the lower layer when the wind is strong. Therefore, a methane burst is expected to occur not only in meromictic lakes but also in stratified freshwater lakes, which means that a methane burst may be a critical event for global warming. Thus, the method used in this study should be applied to investigate how much methane flux is released from eutrophic freshwater lakes around the world.

Methane bursts are caused by wind-induced upwelling, and there have been many studies on upwelling (Watson, 1904; Wedderburn, 1912). Imberger (1998) showed that wind-induced motions, such as blue tides, are ecologically crucial for flux paths. Thompson and Imberger (1980) introduced the Wedderburn number, which shows the magnitude of upwelling in a rectangular lake (Imberger and Hamblin, 1982). Monismith (1986) also demonstrated the importance of the entrainment of hypolimnetic water into the upper layer due to upwelling (burst). Additionally, Shintani et al. (2010) proposed the modified Wedderburn number for evaluating upwelling due to strong wind in a triangle-shaped lake. According to the Intergovernmental Panel on Climate Change (IPCC, 2013) Fifth Assessment Report (AR5) and related papers, not only air temperature but also wind speed may increase in the near future, such as during an extreme event (Nakayama et al., 2010; Nakayama et al., 2013). The present study revealed that strong stratification might accumulate a higher concentration of DM in the lower layer of a eutrophic lake due to the suppression of vertical scalar transport in a density interface and to the inhibition of the oxidation. Thus, it may be expected that methane bursts could occur more often in the future and accelerate climate change, which may in turn cause larger floods and disasters. Therefore, the prediction of changes for disaster prevention depends on how well detailed processes related to methane production and emission from lakes are clarified.

References
Bastviken, D., J. Ejkertsson, and L. Tranvik., 2002. Measurement of methane oxidation in lakes: a comparison of methods. Environ. Sci. Technol. 36, 3354-3361.
Bastviken, D., Cole, J.J., Pace, M.L., Tranvik, L., 2004. Methane emissions from lakes: Dependence of lake characteristics, two regional assessments, and a global estimate. Global Biogeochem. Cycles 18, GB4009, doi:10.1029/2004GB002238
Bastviken, D., Cole, J., Pace, M.L., Van de Boger, M.C., 2008. Fates of methane from different lake habitats: Connecting whole-lake budgets and CH_4 emissions. J. Geophys. Res. 113, G02024, doi:10.1029/2007JG000608
Bocaniov, S.A., Ullmann, C., Rinke, K., Lamb, K.G., Boehrer, B., 2014. Internal waves and mixing in a stratified reservoir: Insights from three-dimensional modeling. Limnologica 49, 52-62, DOI:10.1016/j.limno.2014.08.004

Boetius, A., Ravenschlag, K., Schubert, C.J., Rlckert, D., Wlddel, F., Gleseke, A., Amann, R., Jorgesen, B.B., Wltte, U., Pfannkuche, O., 2000. A marine microbial consortium apparently mediating anaerobic oxidation of methane. Nature 407, 623-626, doi:10.1038/35036572

Capone, D.G., Kiene, R.P., 1988. Comparison of microbial dynamics in marine and freshwater sediments: Contrasts in anaerobic carbon catabolism. Limnol. Oceanogr. 33, 725-749, DOI:10.4319/lo.1988.33.4_part_2.0725

Cole, J.J., Caraco, N.F., 1998. Atmospheric exchange of carbon dioxide in a low-wind oligotrophic lake measured by the addition of SF_6. Limnol. Oceanogr. 43(4), 647-656, https://doi.org/10.4319/lo.1998.43.4.0647

Finlay, K.P., Cyr, H., Shuter, B.J., 2001. Spatial and temporal variability in water temperatures in the littoral zone of a multibasin lake. Can. J. Fish. Aquat. Sci. 58, 609–619, doi:10.1139/cjfas-58-3-609

Imberger, J., 1998. Flux paths in a stratified lake: A review. in Imberger, J. [Ed.], Physical processes in lakes and oceans. Coastal and estuarine studies, American Geophysical Union, pp. 1–18.

Imberger, J., Hamblin, P.F., 1982. Dynamics of lakes, reservoirs and cooling ponds. Annu. Rev. Fluid Mech. 14, 153–187, doi:10.1146/annurev.fl.14.010182.001101.

IPCC, 2013. In: Stocker, T.F., et al. (Eds.), Climate Change 2013: The Physical Science Basis in Contribution of Working Group I to the Fifth Assessment Report of the Intergovernmental Panel on Climate Change (Cambridge and New York).

Juutinen, S., Rantakari, M., Kortelainen, P., Huttunenn, J.T., Larmala, T., Alm, J., Silvola, J., Martikainen, P.J., 2009. Methane dynamics in different boreal lake types. Biogeosciences 6, 209-223, https://doi.org/10.5194/bg-6-209-2009

Leonard, B.P., 1991. The ULTIMATE conservative difference scheme applied to unsteady one-dimensional advection. Comput. Methods Appl. Mech. Eng. 88, 17–74, doi:10.1016/0045–7825(91)90232-U

Liss, P. and Slater, P., 1974. Flux of gases across the air-sea interface. Nature 247, 181-184.

Macintyre, S., Flynn, K.M., Jellison, R., Romero, J., 1999. Boundary mixing and nutrient fluxes in Mono Lake, California. Limnol. Oceanogr. 44, 512–529, https://doi.org/10.4319/lo.1999.44.3.0512

Maruya, Y., Nakayama, K., Shintani, T., Yonemoto, M., 2010. Evaluation of entrainment velocity induced by wind stress in a two–layer system. Hydrol. Res. Lett. 4, 70-74, doi:10.3178/hrl.4.70

Maruya, Y., Nakayama, K., Sasaki, M., Shintani, T., Komai, K., Okada, T., Sugawara, Y., Muneta, N., 2013. Clarification of mechanisms of methane emission in Lake Abashiri. J. Jpn. Soc. Civil Engrs. Ser. B1 (Hydraulic Engineering) 69(4), 1435-1440. (in Japanese)

Maruya, Y., Nakayama, K., Sasaki, M., Komai, K., 2022. Effect of dissolved oxygen on methane production from bottom sediment in a eutrophic stratified lake. J. Environ. Sci., https://doi.org/10.1016/j.jes.2022.01.025.

Minami, H., Tatsumi, K., Hachikubo, A., Yamashita, S., Sakagami, H., Takahashi, N., Shoji, H., Jin, Y.K., Obzhirov, A., Nikolaeva, N., Derkachev, A., 2012. Possible variation in methane flux caused by gas hydrate formation on the northeastern continental slope off Sakhalin Island, Russia. Geo-Mar. Lett. 32, 525-534, DOI 10.1007/s00367-012-0287-x

Miura, S., Hotta, T., Negishi, H., Tsuruta, Y., 2009. Research and analysis on generation mechanism of blue-tide in urban river estuary, Annu. J. Hydraul. Eng. JSCE. 53, 1453-1458. (in Japanese)

Ministry of Land, Infrastructure, Transport and Tourism, 2007. In: Fukuoka, S. et al. (Eds.), Technical report of Ministry of Land, Infrastructure, Transport and Tourism: Hydraulics and water quality control in lakes.

http://www.mlit.go.jp/river/shishin_guideline/kankyo/kankyou/kosyo/tec/ (accessed 8 December 2021). (in Japanese)

Monismith, S.G., 1986. An experimental study of the upwelling response of stratified reservoirs to the surface shear stress. J. Fluid Mech. 171, 407–439, doi:10.1017/S0022112086001507

Nakayama, K., 2006. Comparisons of using CIP, compact and CIP-CSL2 schemes for internal solitary waves. Int. J. Numer. Method F. 51, 197–219, doi:10.1002/fld.1112

Nakayama, K., Imberger, J., 2010. Residual circulation due to internal waves shoaling on a slope. Limnol. Oceanogr. 55(3), 1009–1023, https://doi.org/10.4319/lo.2010.55.3.1009

Nakayama, K., Sivapalan, M., Sato, C., Furukawa, K., 2010. Stochastic characterization of the onset of and recovery from hypoxia in Tokyo Bay, Japan: Derived distribution analysis based on "strong wind" events. Water Resour. Res. 46, W12532, https://doi.org/10.1029/2009WR008900

Nakayama, K, Shintani, T., Kokubo, K., Kakinuma, T., Maruya, Y., Komai, K., 2012. Residual currents over a uniform slope due to breaking of internal waves in a two-layer system. J. Geophys. Res. 117, C10002, doi:10.1029/2012JC008155

Nakayama, K., Maruya, Y., Nakaegawa, T., Komai, K., Kokubo, K., Ishida, T., Okada, T., 2013. Projection of "strong wind" events related to recovery from hypoxia in Tokyo Bay, Japan. Hydrol. Process. 27, 3280-3291, https://doi.org/10.1002/hyp.9829

Nakayama, K., Shintani, T., Shimizu, K., Okada, T., Hinata, H., Komai, K., 2014. Horizontal and residual circulations driven by wind stress curl in Tokyo Bay. J. Geophys. Res. 119, 1977-1992, doi: 10.1002/2013JC009396

Nakayama, K., Nguyen, H.D., Shintani, T., Komai, K., 2016. Reversal of secondary circulations in a sharp channel bend. Coas. Eng. J. 58, 1650002, https://doi.org/10.1142/S0578563416500029

Nakayama, K., Sato, T., Shimizu, K., Boegman, L., 2019. Classification of internal solitary wave breaking over a slope. Phys. Rev. Fluids, 4, 014801, DOI: 10.1103/PhysRevFluids.4.014801

Nakayama, K., Nakagawa, Y., Nakanishi, Y., Kuwae, T., Watanabe, K., Moki, H., Komai, K., Tada, K., Tsai, J.W., Hipsey, M.R., 2020a. Integration of submerged aquatic vegetation motion within hydrodynamic models. Water Resour. Res. 56, e2020WR027369, https://doi.org/10.1029/2020WR027369

Nakayama, K., Sato, T., Tani, K., Boegman, L., Fujita, I., 2020b. Breaking of internal Kelvin wave shoaling on a slope. J. Geophys. Res. 125(10), e2020JC016120, https://doi.org/10.1002/essoar.10502329.1

Postgate, J.R., 1979. The sulfate-reducing bacteria, Cambridge University Press.

Reynolds, C.S., 2006. Ecology of plankton, Cambridge University Press.

Sasaki, J., Kawamoto, S., Yoshimoto, Y., Ishii, M., Kakino, J., 2009. Evaluation of the amount of hydrogen sulfide in a dredged trench of Tokyo Bay. J. of Coast. Res., SI 56, Proc. of the 10th Intern. Coast. Symp. 890-894.

Sasaki, M., Endoh, N., Imura, S., Kudoh, S., Yamanouchi, T., Morimoto, S., Hashida, G., 2010. Air-lake exchange of methane during the open water season in Syowa Oasis, East Antarctica. J. Geophys. Res. 115, D16313, doi:10.1029/2010JD013822

Sasaki, M., Endoh, N., 2014. Exchanges of methane between lakes and the atmosphere in Hokkaido, Subarctic Climate Region, Japan. J. Water Resour. Ocean Sci. 3, 89-94, doi: 10.11648/j.wros.20140306.14

Sasaki, M., Kim, Y.-W., Uchida, M., Utsumi, M., 2016. Diffusive summer methane flux from lakes to the atmosphere in the Alaskan arctic zone. Polar Sci. 10, 303–311, doi: 10.1016/j.polar.2016.06.010

Shintani, T., A de la Fuente Nino, Y., Imberger J. 2010. Generalizations of the Wedderburn number: Parameterizing upwelling in stratified lakes. Limnol. Oceanogr. 55, 1377–1389, doi: 10.4319/lo.2010.55.3.1377

Spigel, R.H., Imberger, J., 1980. The classification of mixed layer dynamics in lakes of small to medium size. J. Phys. Oceanogr. 10, 1104–1121, doi:10.1175/1520-0485(1980)010,1104:TCOMLD.2.0.CO;2

Thompson, R.O.R.Y., Imberger, J., 1980. Response of a numerical model of a stratified lake to wind stress. Proc. Int. Symp. Stratified Flows 2, 562–570.

Touma, J.S., 1977. Dependence of the Wind Profile Power Law on Stability for Various Locations. J. Air Pollut. Control Assoc. 27(9), 863-866, DOI:10.1080/00022470.1977.10470503

Umlauf, L., Burchard, H., 2003. A generic length-scale equation for geophysical turbulence models. J. Mar. Res. 61, 235-265, https://doi.org/10.1357/002224003322005087

Warner, J.C., Sherwood, C.R., Arango, H.G., Signell, R.P., 2005. Performance of four turbulence closure models implemented using a generic length scale method. Ocean Model. 8, 81-113, https://doi.org/10.1016/j.ocemod.2003.12.003

Watson, E.R. 1904. Movements of the waters of loch ness, as indicated by temperature observations. Geog. J. 24, 430–437, doi:10.2307/1775951

Watson, A., Nedwell, D.B., 1998. Methane production and emission from peat: the influence of anions (sulphate, nitrate) from acid rain. Atmos. Environ. 32, 3239-3245, DOI:10.1016/S1352-2310(97)00501-3.

Wedderburn, E.M. 1912. Temperature observation in Loch Earn with a further contribution to the hydrodynamical theory of temperature seiches. Earth Environ. Sci. Trans. R. Soc. Edinb. 48, 629–695, DOI: https://doi.org/10.1017/S0080456800015842

Yamamoto, J., Sakou, A., Watanabe, M., Makita, Y., Tanaka, H., 2009. Field observation of anoxic water behavior in the destratification process in Lake Notoro. J. Jpn. Soc. Civil Engrs. B2 (Coast. Eng.) 65(1), 966-970. (in Japanese)

List of table
Table 1
Vertical distributions of limnological characteristics at the center of Lake Abashiri (St.5) on September 29, 2008. temp.: water temperature, COD: chemical oxygen demand, BOD: biological oxygen demand, T-P: total phosphorous, T-N: total nitrogen, S^{2-}: sulfide ion, Chl-a: chlorophyll a, DOC: dissolved organic carbon

| depth	temp.	pH	COD	BOD	T-P	T-N	S^{2-}	Chl-a	DOC
m		-	mg L^{-1}	mg L^{-1}	mg L^{-1}	mg L^{-1}	mg L^{-1}	μg L^{-1}	mg L^{-1}
0.5	15.9	8.5	5.3	1.9	0.05	0.43	0	6.5	3
1	15.9	8.6	4.7	2	0.053	0.42	0	7.2	3
2	15.8	8.6	4.7	1.8	0.052	0.4	0	6.8	3.2
3	15.6	8.5	4.5	1.8	0.058	0.4	0	6.6	3
4	15.5	8.4	4.1	1.5	0.047	0.38	0	6.9	3
5	17.3	7.6	14	4.6	1.3	3.7	8.2	0	4.2
6	16.5	7.5	23	19	1	4.2	25	0	3.4
7	13.7	7.5	36	23	1.6	7.1	39	0	4.2
8	11.4	7.5	42	37	2.1	10	56	0	4.2
9	10.2	7.4	46	46	2.3	11	72	0	4.2
10	8.8	7.3	52	48	2.9	14	85	0	5
11	8.4	7.3	76	62	3.3	17	100	0	5.6
12	8.2	7.3	87	67	3.6	17	110	0	6
13	8.1	7.2	100	75	3.5	17	120	0	5.8
14	8.1	7.2	110	69	3.7	16	110	0	7
15	7.9	7.2	110	72	3.6	18	110	0	6.8
15.5	7.9	7.2	110	75	3.6	17	110	0	6.6
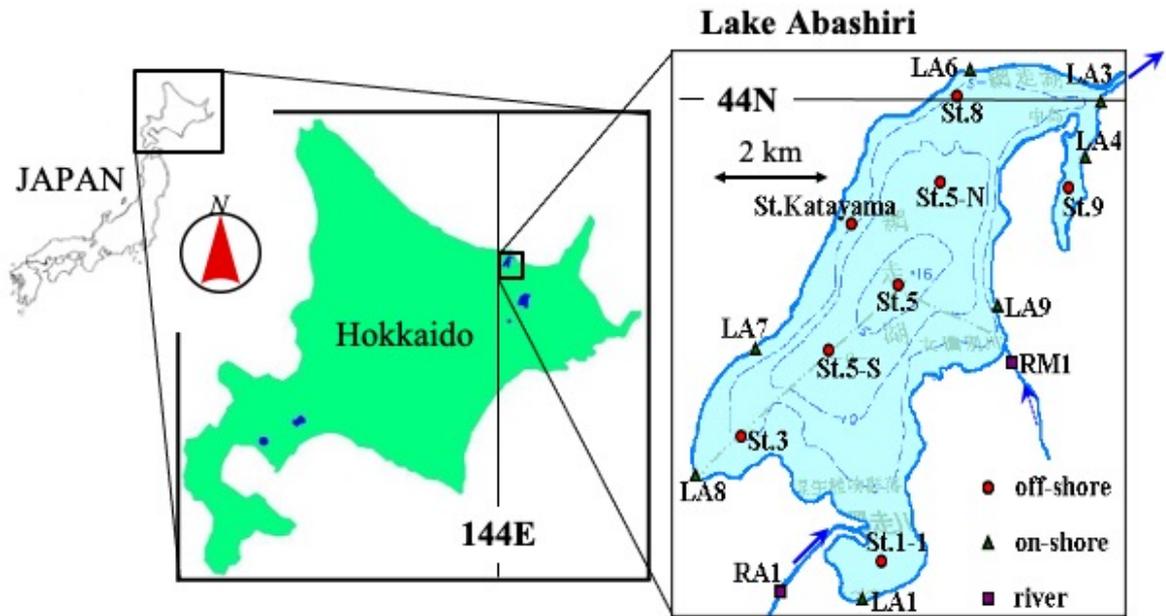
Fig. 1 Location of Lake Abashiri and the observation stations (43°58' north latitude, 144°10' east longitude).
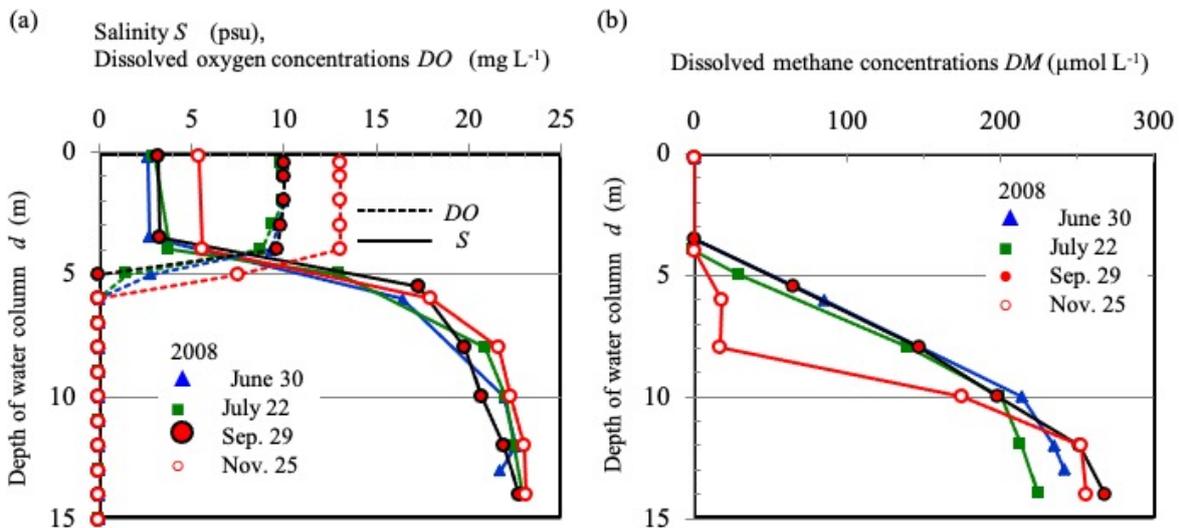

Fig. 2 Vertical profiles of (a) salinity and dissolved oxygen concentrations *DO* at St-5 in 2008, and (b) dissolved methane concentrations *DM* in 2008. Data from September 29, 2008 were applied as the initial condition for numerical computations.
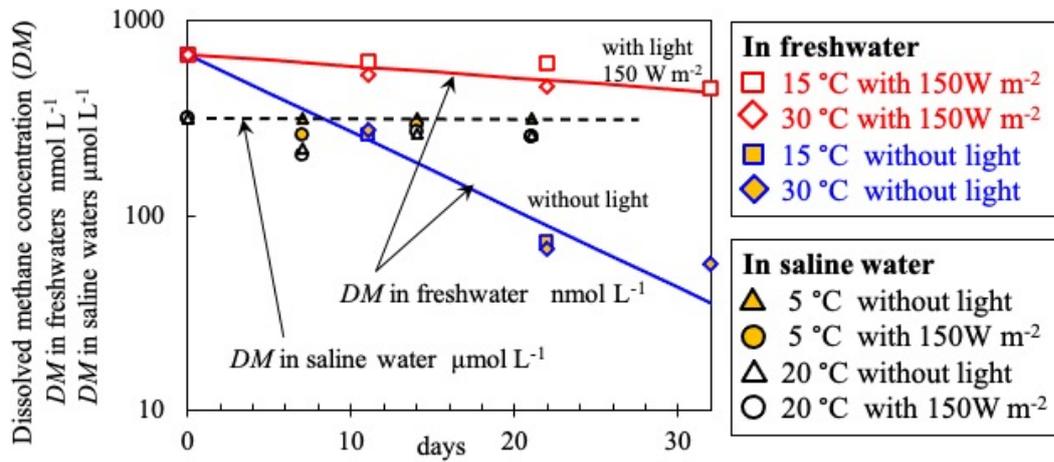
Fig. 3 Time series of DM at cultivation tests. Solid lines indicate freshwater samples obtained at station LA8 from the water surface on June 28, 2010. The dashed line indicates a saline water sample obtained at a depth of 10 m at St. 5 on November 26, 2012.
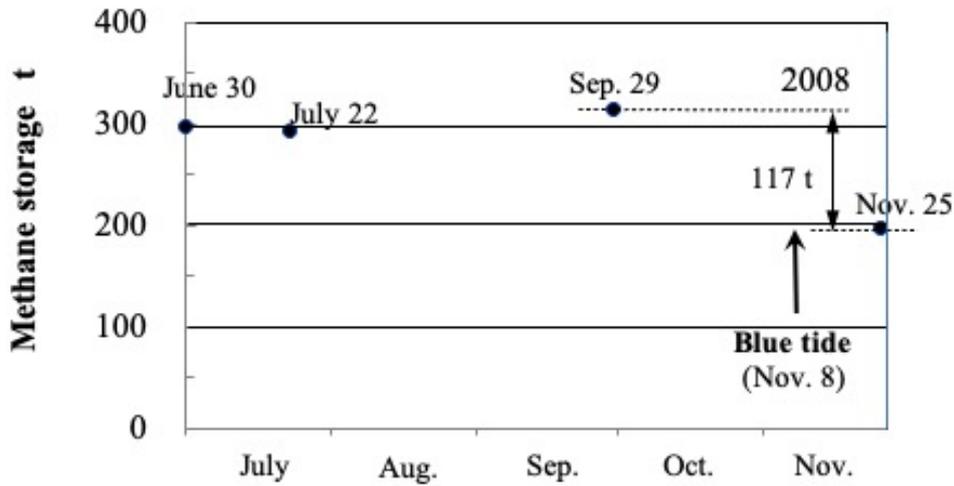
Fig. 4 Methane storage in the saline water layer in Lake Abashiri in 2008.
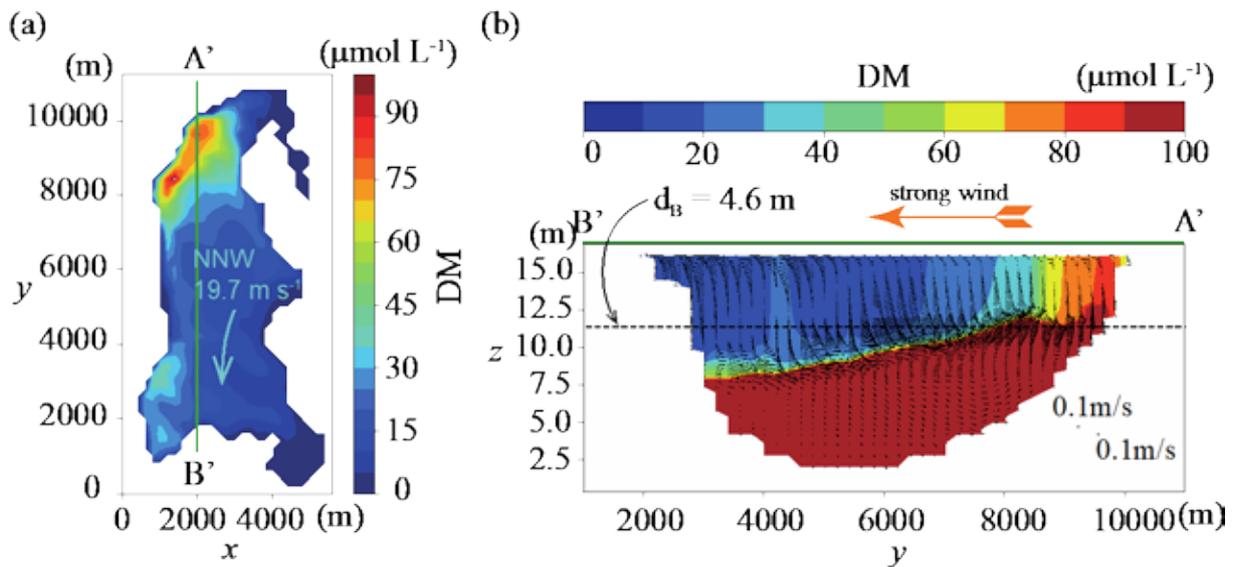

Fig. 5 Velocity and dissolved methane concentration (DM) distributions at the peak of the blue tide at 21:00 JST on November 8, 2008 (circle in **Fig. 8**). dB is the saline water boundary. (a) Horizontal distribution of DM at the water surface. (b) Vertical distribution of DM along the line A'-B'.
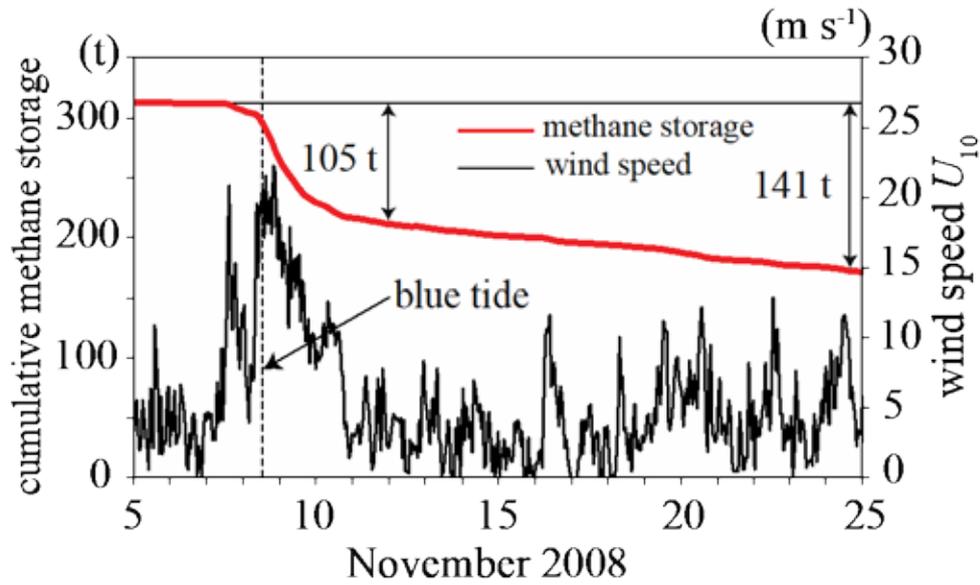
Fig. 6 Cumulative methane transportation from the saline layer to the freshwater layer during the blue tide from November 5 to 10, 2008.
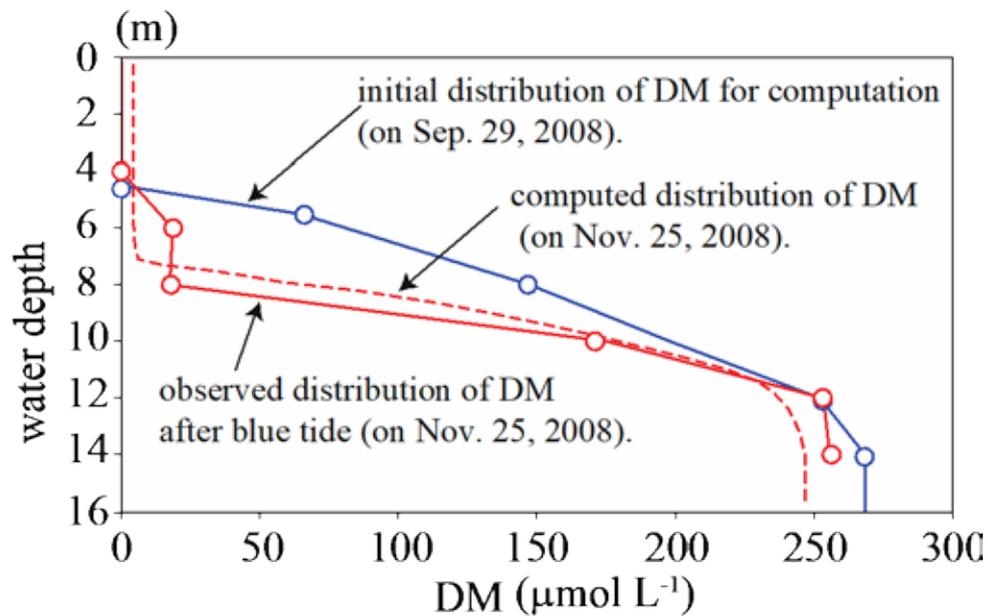

Fig. 7 Vertical profiles of DM. The solid blue line indicates initial conditions for numerical computations observed on September 29, 2008, the solid red line indicates the observed DM on November 25, 2008, and the broken red line indicates the computational result of DM by applying methane flux computations between the water surface and atmosphere on November 25, 2008.
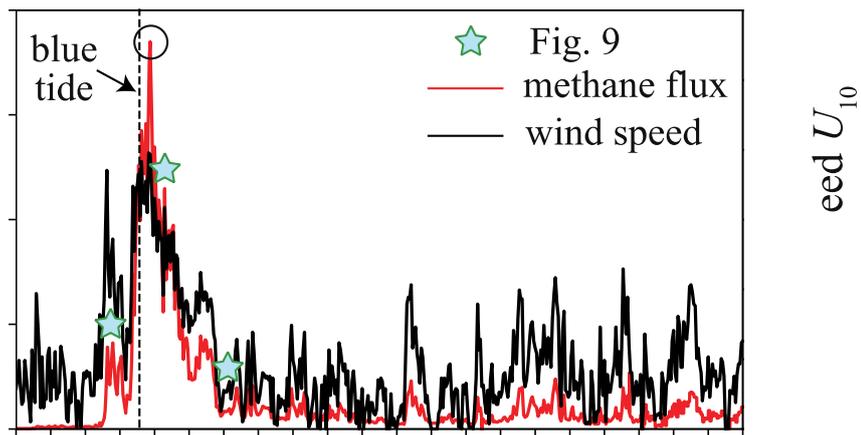
Fig. 8 Methane flux to the atmosphere during the blue tide in 2008. The circle indicates the maximum methane flux shown in **Fig. 5**. Stars correspond to **Fig. 9** at 22:00 on the 7th, 4:00 on the 9th, and 24:00 on the 10th of November, 2008.
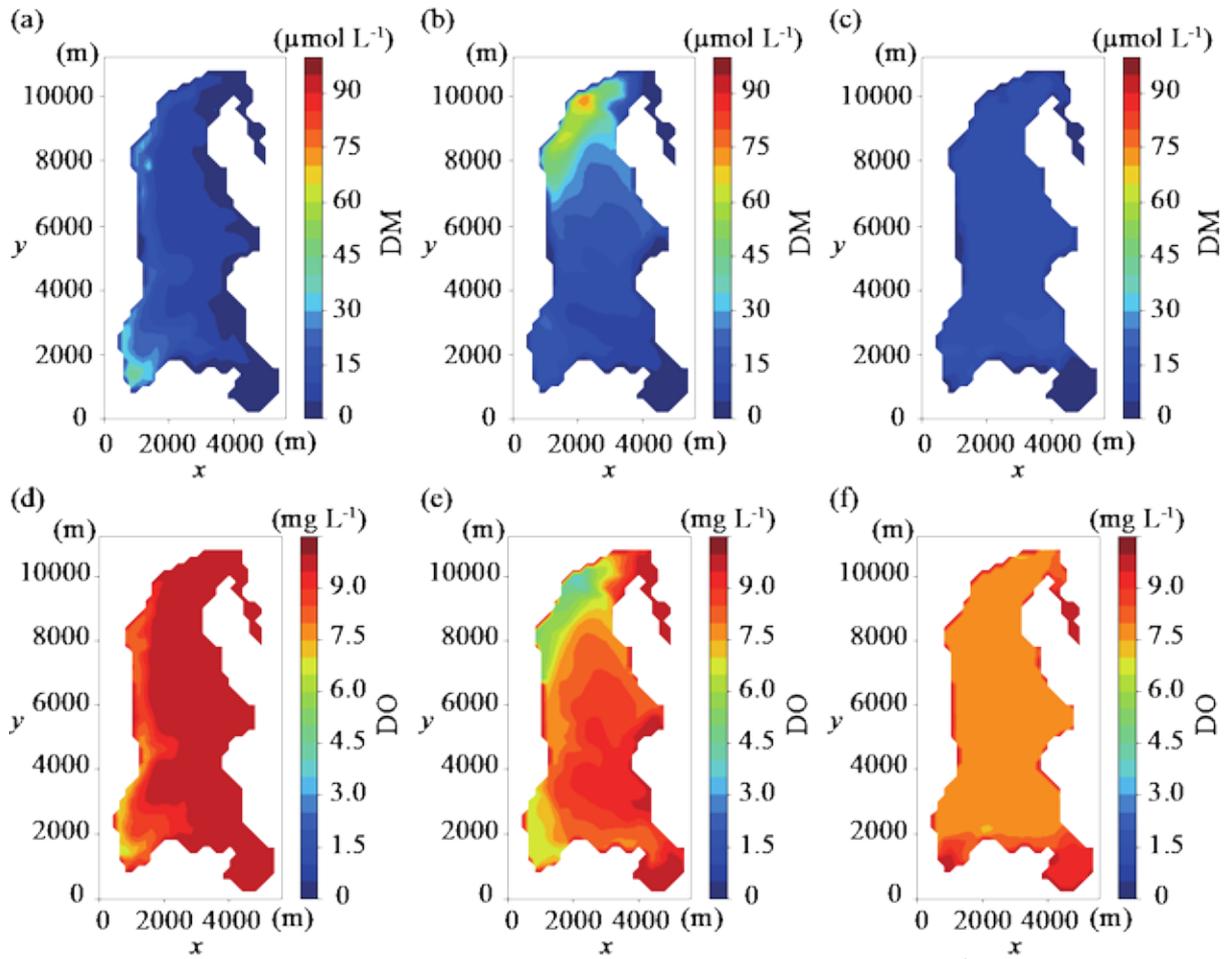
Fig. 9 Horizontal distribution of DM (stars in **Fig. 8**) (a) at 22:00 on the 7th, (b) at 4:00 on the 9th, and (c) at 24:00 on the 10th of November, 2008. Horizontal distribution of DO (d) at 22:00 on the 7th, (e) at 4:00 on the 9th, and (f) at 24:00 on the 10th of November, 2008.
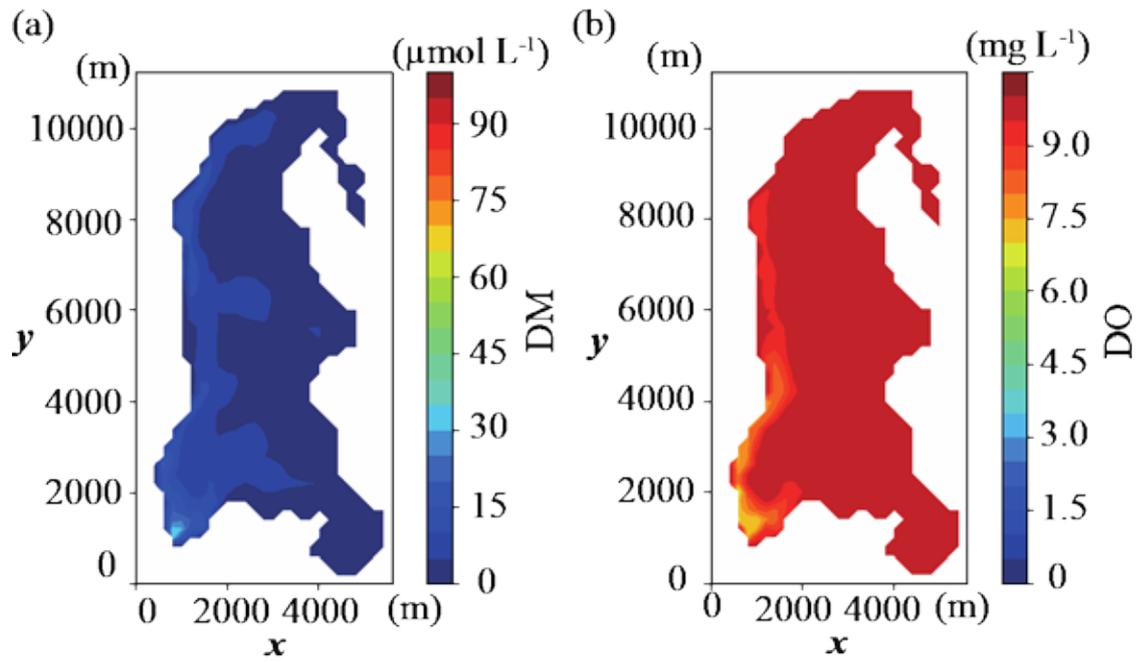
Fig. 10 Horizontal distribution of DM (a) and horizontal distribution of DO (b) at the lake surface, when the depth of the boundary between fresh and saline water is deeper (dB = 6.6 m) at 4:00 on November 9, 2008.